

See discussions, stats, and author profiles for this publication at: <https://www.researchgate.net/publication/6553318>

# Synthesis and Pharmacophore Modeling of Naphthoquinone Derivatives with Cytotoxic Activity in Human Promyelocytic Leukemia HL-60 Cell Line

ARTICLE *in* JOURNAL OF MEDICINAL CHEMISTRY · FEBRUARY 2007

Impact Factor: 5.45 · DOI: 10.1021/jm060849b · Source: PubMed

---

CITATIONS

59

---

READS

96

## 7 AUTHORS, INCLUDING:



**Perez Elisa**

Universidad de La Laguna

10 PUBLICATIONS 342 CITATIONS

SEE PROFILE



**Ana Estévez-Braun**

Universidad de La Laguna

90 PUBLICATIONS 1,233 CITATIONS

SEE PROFILE



**Leonardo Pardo**

Autonomous University of Barcelona

115 PUBLICATIONS 3,894 CITATIONS

SEE PROFILE



**Mercedes Campillo**

Autonomous University of Barcelona

81 PUBLICATIONS 1,681 CITATIONS

SEE PROFILE

## Synthesis and Pharmacophore Modeling of Naphthoquinone Derivatives with Cytotoxic Activity in Human Promyelocytic Leukemia HL-60 Cell Line

Elisa Pérez-Sacau,<sup>†,‡</sup> Raquel G. Díaz-Peñate,<sup>‡,§</sup> Ana Estévez-Braun,<sup>\*,†,‡</sup> Angel G. Ravelo,<sup>\*,†,‡</sup> Jose M. García-Castellano,<sup>‡,§</sup> Leonardo Pardo,<sup>||</sup> and Mercedes Campillo<sup>\*,||</sup>

*Instituto Universitario de Bio-Organica "Antonio González", Universidad de La Laguna, Avda. Astrofísico Fco. Sánchez 2, 38206 La Laguna, Tenerife, Spain, Instituto Canario de Investigaciones del Cáncer, Unidad de Investigación, Hospital de Gran Canaria "Dr. Negrín", Las Palmas de Gran Canaria, and Laboratori de Medicina Computacional, Unitat de Bioestadística, Facultat de Medicina, Universitat Autònoma de Barcelona, Barcelona, Spain*

Received July 20, 2006

Catalyst/HypoGen pharmacophore modeling approach and three-dimensional quantitative structure–activity relationship (3D-QSAR)/comparative molecular similarity indices analysis (CoMSIA) methods have been successfully applied to explain the cytotoxic activity of a set of 51 natural and synthesized naphthoquinone derivatives tested in human promyelocytic leukemia HL-60 cell line. The computational models have facilitated the identification of structural elements of the ligands that are key for antitumoral properties. The four most salient features of the highly active  $\beta$ -cycled-pyran-1,2-naphthoquinones [ $0.1 \mu\text{M} < \text{IC}_{50} < 0.6 \mu\text{M}$ ] are the hydrogen-bond interactions of the carbonyl groups at C-1 (HBA1) and C-2 (HBA2), the hydrogen-bond interaction of the oxygen atom of the pyran ring (HBA3), and the interaction of methyl groups (HYD) at the pyran ring with a hydrophobic area at the receptor. The moderately active 1,4-naphthoquinone derivatives accurately fulfill only three of these features. The results of our study provide a valuable tool in designing new and more potent cytotoxic analogues.

### Introduction

Cancer is, in the developed world, the second most common cause of death after cardiovascular diseases.<sup>1</sup> Mass screening programs of natural products by the National Cancer Institute have identified the quinone moiety as an important pharmacophoric element for cytotoxic activity.<sup>2</sup> Lapachol **1** and several natural related 1,4- and 1,2-naphthoquinones are associated with numerous biological activities<sup>3</sup> like antibacterial,<sup>4</sup> fungicidal,<sup>4</sup> antimalarial,<sup>5</sup> trypanocidal,<sup>6</sup> and antitumoral.<sup>7</sup> On the basis of the biological and structural properties, 1,2- and 1,4-naphthoquinones are considered privileged structures in medicinal chemistry.<sup>8</sup> This term describes selected structural types like polycyclic heteroatomic systems, capable of orienting varied substituent patterns in a well-defined three-dimensional space and binding to multiple, unrelated classes of protein receptors as high-affinity ligands.

The most important lapachol derivative with antitumoral activity is  $\beta$ -lapachone (3,4-dihydro-2,2-dimethyl-2*H*-naphtho-[1,2-*b*]pyran-5,6-dione) **15**. This compound induces cell death in human cancer cells<sup>9</sup> without causing direct damage to DNA,<sup>10</sup> showing low effect on nontumoral proliferative cells.<sup>11</sup>  $\beta$ -Lapachone also has potent antitumor activity in xenografted human cancer models with low host toxicity.<sup>9a</sup>

Although the  $\beta$ -lapachone cytotoxic action has been known for more than 20 years,<sup>12</sup> the detailed mechanism of action has yet to be investigated. The first proposed biochemical target for  $\beta$ -lapachone was DNA topoisomerase I,<sup>13</sup> being the unique drug that binds to the enzyme and inhibits its catalytic activity

without stabilizing the DNA–enzyme complex. The enzyme NAD(P)H:quinone oxidoreductase (NQO1, Xip3, E.C. 1.6.99.2), a ubiquitous flavoprotein found in most eukaryotes, is also key for the action of  $\beta$ -lapachone.<sup>9b</sup> NQO1 catalyzes a two-electron reduction of quinones, like  $\beta$ -lapachone or menadione, using either NADH or NADPH as electron donor. Reduction of  $\beta$ -lapachone by NQO1 increases its cytotoxic action, including growth inhibition and apoptotic proteolysis. NQO1 is overexpressed in breast, colon, lung, and prostate tumors,<sup>14</sup> making  $\beta$ -lapachone or/and its derivatives a potential therapeutic agent for these kinds of tumors.<sup>15</sup> However,  $\beta$ -lapachone elicits different responses in cells with similar expression levels of NQO1, such as NCM460 and SW480, or it elicits apoptosis in cells lacking NQO1, such as HL-60 and MDAMB-468.<sup>9b</sup> In the human cell line HL60, derived from a promyelocytic leukemia,  $\beta$ -lapachone induces apoptosis by a reactive oxygen species (ROS) and JNK-dependent pathway<sup>16</sup> and in a p53-independent manner.<sup>17</sup> These findings suggest that the antitumor activity of  $\beta$ -lapachone is induced by different mechanisms of action depending on the tumor cell type.

Presently, the structural requirements of quinone derivatives inducing apoptosis are unknown, hampering the rational development of new specific compounds. A pharmacophore definition is known as the first essential step toward understanding the interaction between a ligand and its target, and it is clearly established as a successful computational tool for rational drug design.<sup>18</sup> In the present work, with the aim of gaining insight into the molecular determinants of action of this type of compound, we have developed a pharmacophore model using the Catalyst program (Catalyst, version 4.10; Molecular Simulations Inc.: San Diego, CA, 2005) as a systematic and efficient procedure. In addition, we have performed complementary three-dimensional quantitative structure–activity relationship (3D-QSAR) analysis<sup>19</sup> based on comparative molecular similarity indices analysis (CoMSIA) studies.<sup>20</sup> These methodologies were applied to a set of 51 bioactive naphthoquinones (NQ) tested

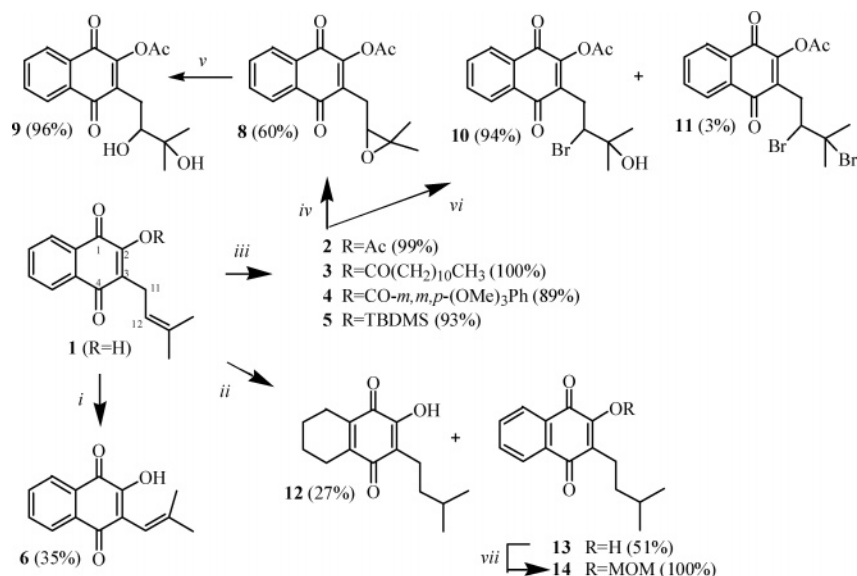
\* To whom correspondence should be addressed: phone + 34 922 318576 (A.E.-B., A.G.R.), + 34 935 812348 (M.C.); fax + 34 922 318571 (A.E.-B., A.G.R.), + 34 935 812344 (M.C.); e-mail aestebra@ull.es (A.E.-B.), agravelo@ull.es (A.G.R.), mercedes.campillo@uab.es (M.C.).

<sup>†</sup> Universidad de La Laguna.

<sup>‡</sup> Instituto Canario de Investigaciones del Cáncer (<http://www.icic.es>).

<sup>§</sup> Hospital de Gran Canaria "Dr. Negrín".

<sup>||</sup> Universitat Autònoma de Barcelona.

**Scheme 1.** Synthesis of 1,4-Naphthoquinone Derivatives<sup>a</sup>

in a cytotoxicity assay on HL-60 cells to provide important information on the active site of the target protein where these NQ elicit their functions.

## Results

**Chemistry.** Most of the derivatives were obtained from lapachol **1** and lawsone **53**, which are bioactive naphthoquinones isolated from plants of the Bignoniaceae family. They are also easily available commercial products.

(A) Synthesis of 1,4-Naphthoquinone Derivatives (Scheme 1). Compounds **2**–**4** were obtained from lapachol **1** by employing a variety of acylating agents of different electrophilicity and lipophilicity in the presence of 2,6-lutidine as base. Compound **5** was achieved by treatment of **1** with the voluminous *tert*-butyldimethylsilyl chloride, with triethylamine as base. Compound **6**, with a shorter side chain, was synthesized by Hooker's oxidation<sup>5b</sup> of **1**. Derivatives **8**–**11** were also synthesized in order to study the role of the side chain in their cytotoxic activity. They were obtained by modifications of the exocyclic double bond of derivative **2**. Thus, compound **2** was treated with *m*-CPBA to obtain the corresponding ( $\pm$ )-epoxy derivative **8** in 60% yield, which, under treatment with  $\text{HClO}_4$  in catalytic amounts, afforded diol **9** in 96% yield. In addition, the reaction of **2** with *N*-bromosuccinimide (NBS) in  $^t\text{BuOH}/\text{H}_2\text{O}$  (1/1) yielded compound **10** (94%) and the dibromo derivative **11** (3%). Hydrogenation of **1** with  $\text{H}_2/\text{Pd}$  afforded compounds **12** and **13**, the first one exhibiting a partial reduction of the A ring. Treatment of **13** with methoxymethylchloride (MOMCl) produced compound **14**, which contains a methoxymethyl ether group at position C-2.

(B) Synthesis of Prenyl Pyran and Furan Naphthoquinones (Scheme 2). Treatment of **1** with diluted  $\text{H}_2\text{SO}_4$  produces a tertiary carbocation that is intramolecularly trapped by the hydroxyl group located on carbon C-2 or by the oxygen located at C-4, yielding  $\beta$ -lapachone **15** (angular tricyclic derivative) and  $\alpha$ -lapachone **36** (linear tricyclic derivative), respectively.<sup>21</sup> Cyclization of **1** with *m*-chloroperoxybenzoic acid (*m*-CPBA), via an epoxide intermediate, rendered the furan and pyran naphthoquinones **18**, **30**, **32**, and **52** in their racemic forms. Reaction of **1** with 2 equiv of ammonium cerium(IV) nitrate

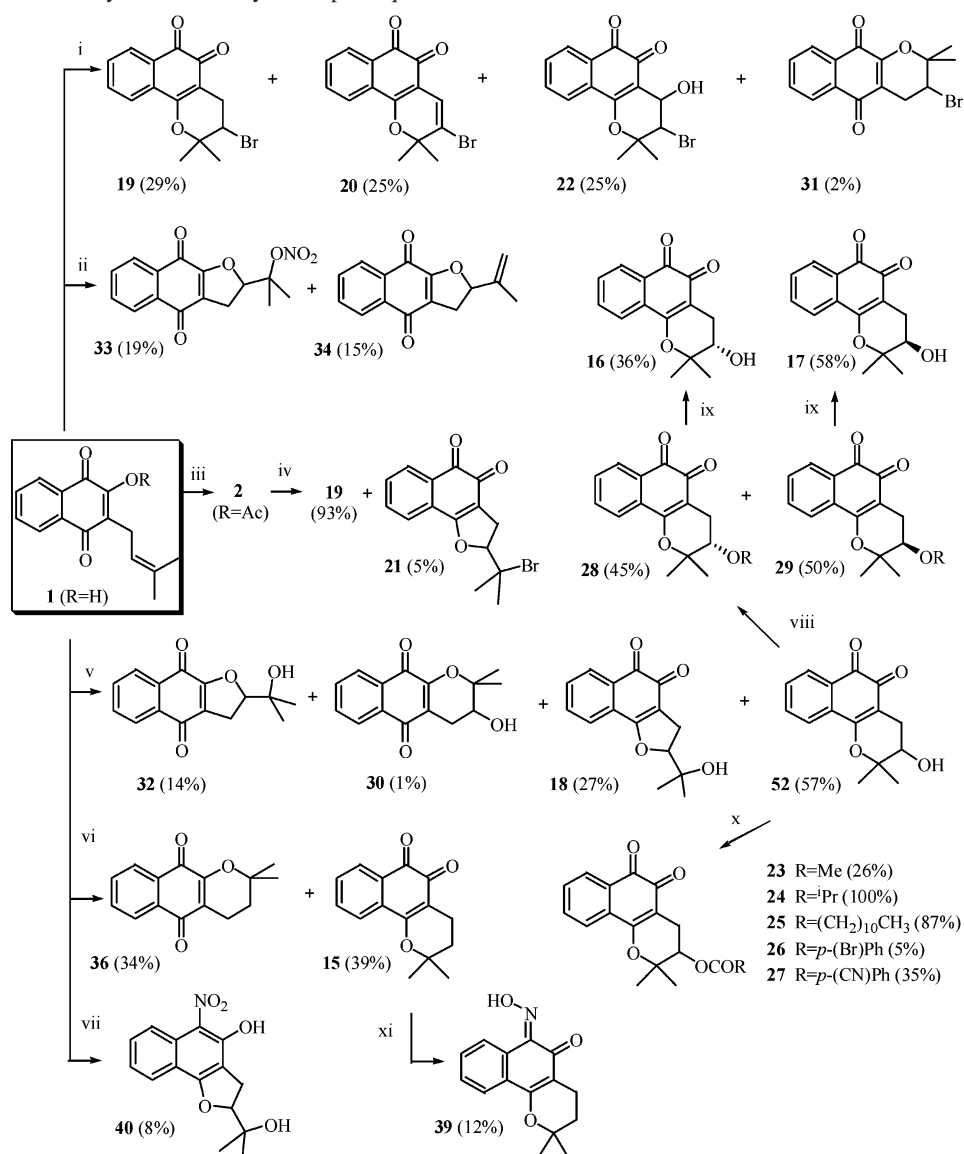
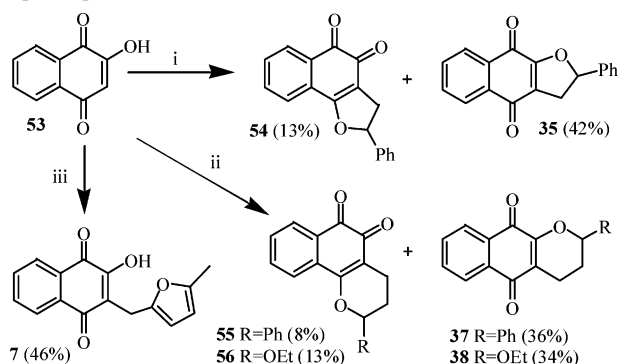
$[(\text{NH}_4)_2\text{Ce}(\text{NO}_3)_6]$  yielded the linear furan naphthoquinones **33** and **34**. Treatment of **1** with NBS in  $\text{CH}_2\text{Cl}_2$  afforded compounds **19**, **20**, **22**, and **31**. Compound **19** was also obtained in higher yield (93%) from **2** and  $\text{Br}_2/\text{CH}_2\text{Cl}_2$ . This reaction also afforded the  $\beta$ -furan isomer **21** as a minor compound.

The ( $\pm$ ) ester derivatives **23**–**27** were synthesized from the racemic alcohol **52** by employing a variety of acylating agents such as acetyl, isopropyl, lauroyl, *p*-bromobenzoyl, and *p*-cyanobenzoyl chlorides. The stereoisomers **28** and **29** were obtained from the esterification of **52** with (*R*)- $\alpha$ -methoxyphenylacetic acid in the presence of DCC (dicyclohexylcarbodiimide) and catalytic amounts of DMAP (dimethylaminopyridine). The absolute configuration of these compounds was established by following the method described by Riguera and co-workers.<sup>22</sup> The enantiomeric alcohols **16** and **17** were obtained by mild basic hydrolysis of the corresponding esters **28** and **29** with  $\text{NaHCO}_3/\text{MeOH}$  at rt.

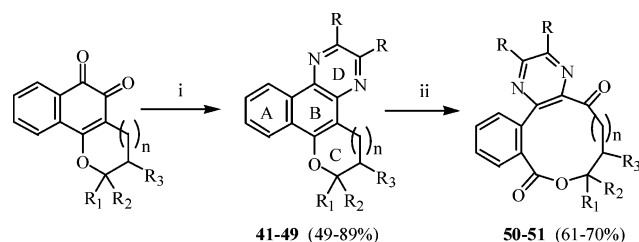
Reaction of compound **15** with hydroxylamine hydrochloride ( $\text{NH}_2\text{OH}\cdot\text{HCl}$ ) provided the oxime **39** in a regioselective form. Compound **40** was obtained from **1**, under treatment with  $\text{NH}_2\text{OH}\cdot\text{HCl}$  and posterior cyclization with *m*-CPBA. The formation of the nitro derivative **40** can be due to the formation of a nitroso-phenol intermediate and a posterior oxidation with *m*-CPBA.

(C) Synthesis of Non-prenyl Pyran and Furan Naphthoquinones (Scheme 3). Compound **35** was obtained by treatment of lawsone **53** with ceric ammonium nitrate (CAN) and styrene in aqueous acetonitrile at  $0^\circ\text{C}$ , via [3 + 2]-type cycloaddition. The Knoevenagel condensation of lawsone **53** and paraformaldehyde  $(\text{CH}_2\text{O})_n$  leads to a quinone methide intermediate, which undergoes hetero Diels–Alder reaction with styrene or ethyl vinyl ether as dienophiles, yielding in a one-pot reaction the pyran naphthoquinones **37** or **38**, respectively. When 2-methylfuran was used as dienophile, compound **7** was formed instead of the expected pyran naphthoquinone derivative. The formation of **7** is the result of an electrophilic substitution on the furan ring, where the quinone methide intermediate acts as electrophile.

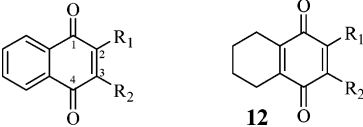
(D) Synthesis of 1,4-Diazaphenanthrene Compounds and 9- and 10-Membered Macrolactones (Scheme 4). 1,4-Diaza-

**Scheme 2.** Synthesis of Prenyl Furan and Pyran Naphthoquinones<sup>a</sup>**Scheme 3.** Synthesis of Non-prenyl Pyran and Furan Naphthoquinones<sup>a</sup>

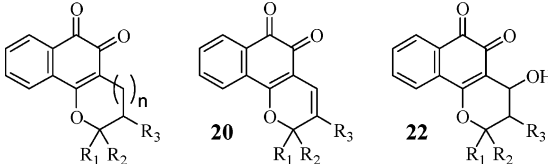
phenanthrene derivatives **41–49** were synthesized by condensation of lapachol **1** and the *o*-quinones **15**, **18**, **19**, **23**, and **52**

**Scheme 4.** Synthesis of Diazaphenanthrene Derivatives and Macrolactones<sup>a</sup>

with 1,2-ethylenediamine or *trans*-1,2-diaminecyclohexane.<sup>23</sup> The treatment of compounds **46** and **49** with ozone produced a selective oxidative cleavage of the enol double bond shared by rings B and C, leading to the corresponding macrolactones **50** and **51**.

**Table 1.** *p*-1,4-Naphthoquinone Derivatives (Bicyclic Compounds)


compd	R <sub>1</sub>	R <sub>2</sub>	IC <sub>50</sub> ± SD (mM)				Δ <i>G</i> <sub>solv</sub> (kcal/mol)	log <i>P</i>
			exptl	rank	est Catalyst	est CoMSIA		
1	OH	CH <sub>2</sub> CH=C(CH <sub>3</sub> ) <sub>2</sub>	3.18 ± 1.1	++	3.0	1.8	−6.1	4.1
2	OAc	CH <sub>2</sub> CH=C(CH <sub>3</sub> ) <sub>2</sub>	4.51 ± 0.8	++	19	8.3	−6.8	4.5
3	OCO(CH <sub>2</sub> ) <sub>10</sub> CH <sub>3</sub>	CH <sub>2</sub> CH=C(CH <sub>3</sub> ) <sub>2</sub>	26.26 ± 1.9	+	10	16	−4.4	9.9
4	OCO- <i>m,m,p</i> -(OMe) <sub>3</sub> Ph	CH <sub>2</sub> CH=C(CH <sub>3</sub> ) <sub>2</sub>	8.06 ± 3.1	++	10	10	−9.5	6.3
5	OTBDMS	CH <sub>2</sub> CH=C(CH <sub>3</sub> ) <sub>2</sub>	11.44 ± 0.6	+	8.1	14	−1.7	7.3
6	OH	CH=C(CH <sub>3</sub> ) <sub>2</sub>	27.74 ± 4.4	+	22	34	−6.7	3.2
7	OH	CH <sub>2</sub> [2-(5-methylfuran)]	68.25 ± 1.3	+	39	62	−10.3	3.6
8	OAc	CH <sub>2</sub> (2,2-dimethyloxirane)	1.89 ± 0.5	++	1.1	2.3	−11.8	3.0
9	OAc	CH <sub>2</sub> CHOHCOH(CH <sub>3</sub> ) <sub>2</sub>	48.12 ± 16.3	+	30	42	−16.1	1.8
10	OAc	CH <sub>2</sub> CHBrCOH(CH <sub>3</sub> ) <sub>2</sub>	0.52 ± 0.4	+++	5.4	−6.5	−13.8	3.5
11	OAc	CH <sub>2</sub> CHBrCBr(CH <sub>3</sub> ) <sub>2</sub>	2.23 ± 1.5	++	3.0	5.4	−10.4	5.1
12	OH	CH <sub>2</sub> CH <sub>2</sub> CH(CH <sub>3</sub> ) <sub>2</sub>	34.60 ± 7.1	+	51	51 <sup>a</sup>	−6.9	4.2
13	OH	CH <sub>2</sub> CH <sub>2</sub> CH(CH <sub>3</sub> ) <sub>2</sub>	62.13 ± 2.9	+	15	66	−8.0	4.1
14	OCH <sub>2</sub> OCH <sub>3</sub>	CH <sub>2</sub> CH <sub>2</sub> CH(CH <sub>3</sub> ) <sub>2</sub>	53.91 (1.6)	+	33	37	−5.8	4.4

<sup>a</sup> Compounds used to test the CoMSIA model.**Table 2.** Pyran- and Furan-1,2-Naphthoquinone Derivatives (β-Cycled, Angular Tricyclic Compounds)


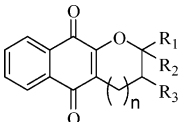
compd	<i>n</i>	R <sub>1</sub>	R <sub>2</sub>	R <sub>3</sub>	IC <sub>50</sub> ± SD (μM)				Δ <i>G</i> <sub>solv</sub> (kcal/mol)	log <i>P</i>
					exptl	rank	est Catalyst	est CoMSIA		
15	1	Me	Me	H	0.27 ± 0.04	+++	0.39	3.7	−7.2	3.2
16	1	Me	Me	OH ( <i>S</i> )	0.57 ± 0.02	+++	0.66	4.9	−11.1	2.2
17	1	Me	Me	OH ( <i>R</i> )	0.55 ± 0.1	+++	0.52	−3.0	−11.1	2.2
18	0	C(OH)(CH <sub>3</sub> ) <sub>2</sub>	H	H	1.97 ± 0.3	++	3.7	1.6	−11.6	1.6
19	1	Me	Me	Br	0.13 ± 0.02	+++	0.22	0.9	−7.5	3.6
20	1	Me	Me	Br	0.20 ± 0.1	+++	0.17	−0.1 <sup>a</sup>	−7.3	3.5
21	0	C(Br)(CH <sub>3</sub> ) <sub>2</sub>	H	H	0.70 ± 0.2	+++	0.14	6.0	−8.3	3.2
22	1	Me	Me	Br	0.12 ± 0.02	+++	0.19	2.7	−11.7	3.1
23	1	Me	Me	OAc	0.68 ± 0.3	+++	0.22	2.2	−10.9	3.0
24	1	Me	Me	OCOPr <sup>i</sup>	0.24 ± 0.04	+++	0.17	2.1	−9.5	3.8
25	1	Me	Me	OCO(CH <sub>2</sub> ) <sub>10</sub> CH <sub>3</sub>	0.26 ± 0.1	+++	0.15	3.1	−7.4	8.3
26	1	Me	Me	OpBrBz	0.45 ± 0.2	+++	0.19	−0.2	−11.0	5.8
27	1	Me	Me	OpCNBz	0.13 ± 0.1	+++	0.15	0.04	−12.4	4.7
28 ( <i>SR</i> )	1	Me	Me	OCOCH(OCH <sub>3</sub> )(Ph)	0.11 ± 0.01	+++	0.16	0.9	−10.5	5.0
29 ( <i>RR</i> )	1	Me	Me	OCOCH(OCH <sub>3</sub> )(Ph)	0.26 (0.04)	+++	0.14	1.7	−9.8	5.0

<sup>a</sup> Compounds used to test the CoMSIA model.

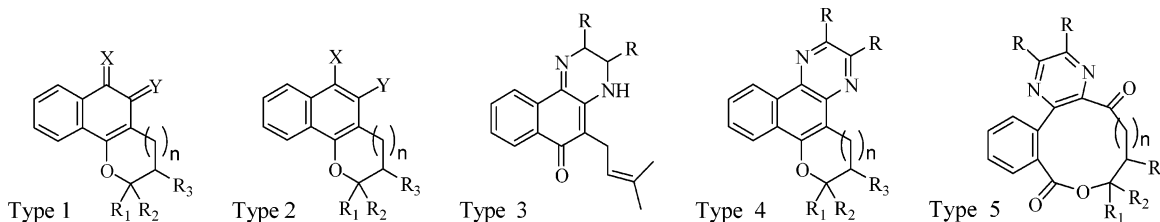
**Biological Assays.** Cytotoxic assays were performed on human promyelocytic leukemia HL-60 cell lines by use of the MTT assay<sup>24</sup> (see Experimental Section). The concentrations inducing a 50% inhibition of cell growth (IC<sub>50</sub>) in μM are reported in Table 1 for *p*-1,4-naphthoquinones (opened derivatives **1–14**); in Table 2 for *o*-1,2-furan and pyran naphthoquinones (β-cycled derivatives **15–29**); in Table 3 for *p*-1,4-furan and pyran naphthoquinones (α-cycled derivatives **30–38**); and in Table 4 for nitrogenous derivatives and 1,4-diazaphenanthrene derivatives (compounds **39–51**). Compounds **1–51** were classified by their activity as highly active (IC<sub>50</sub> < 1 μM, +++), moderately active (1 μM < IC<sub>50</sub> < 10 μM, ++), or inactive (10 μM > IC<sub>50</sub>, +). The most cytotoxic derivatives belong to the *o*-naphthoquinone series (Table 2) with IC<sub>50</sub> values in the 0.1–0.7 μM range, with the only exception being compound **18** (IC<sub>50</sub> = 1.97 μM). Of the other series of compounds, only the bromohydrine derivative **10** shows high activity (IC<sub>50</sub> = 0.52 μM).

**Three-Dimensional Pharmacophore Model for Naphthoquinone Derivatives.** We have developed a three-dimensional pharmacophore model for compounds **1–51** (Tables 1–4) with the Catalyst software. The fixed, null, and configuration costs are 133, 825, and 10 bits, respectively. The difference of 692 bits between fixed and null costs is a sign of highly predictive hypotheses. The average linkage cluster method of Catalyst renders two groups of hypotheses. The hypothesis with the best statistics (total cost of 220 bits) is employed throughout this paper. The statistical significance of this hypothesis was assessed by the Fisher method as implemented in the CatScramble module. The IC<sub>50</sub> values were scrambled randomly 49 times, and new hypotheses were generated. None of the outcome hypotheses had a cost lower than the reported hypothesis (results not shown). Thus, there is at least 98% probability that this hypothesis represents true correlation in the data.<sup>25</sup> Figure 1 shows the structural features of the pharmacophore model consisting of a hydrophobic region (HYD), three hydrogen-



**Table 3.** Pyran- ( $n = 1$ ) and Furan- ( $n = 0$ ) 1,4-Naphthoquinone Derivatives ( $\alpha$ -Cycled, Linear Tricyclic Compounds)


compd	$n$	$R_1$	$R_2$	$R_3$	$IC_{50} \pm SD$ ( $\mu M$ )				$\Delta G_{solv}$ (kcal/mol)	$\log P$
					exptl	rank	est Catalyst	est CoMSIA		
<b>30</b>	1	Me	Me	OH	$1.35 \pm 0.1$	++	4.3	-1.8	-10.2	2.7
<b>31</b>	1	Me	Me	Br	$1.36 \pm 0.4$	++	3.3	-1.3	-6.1	4.1
<b>32</b>	0	$CH(OH)(CH_3)_2$	H	H	$1.85 \pm 0.4$	++	2.1	0.3 <sup>a</sup>	-10.2	2.0
<b>33</b>	0	$CH(ONO_2)(CH_3)_2$	H	H	$1.24 \pm 0.1$	++	1.9	-1.8	-6.7	3.4
<b>34</b>	0	$C(CH_3)=CH_2$	H	H	$1.46 \pm 0.6$	++	2.7	3.4	-6.3	3.4
<b>35</b>	0	Ph	H	H	$2.65 \pm 0.2$	++	7.8	3.7	-8.2	3.7
<b>36</b>	1	Me	Me	H	$13.46 \pm 2.4$	+	10	5.6	-6.0	3.5
<b>37</b>	1	Ph	H	H	$22.91 \pm 3.6$	+	20	26	-6.6	4.7
<b>38</b>	1	OEt	H	H	$29.66 (0.1)$	+	8.7	28	-7.6	2.8

<sup>a</sup> Compounds used to test the CoMSIA model.**Table 4.** Nitrogenous Derivatives


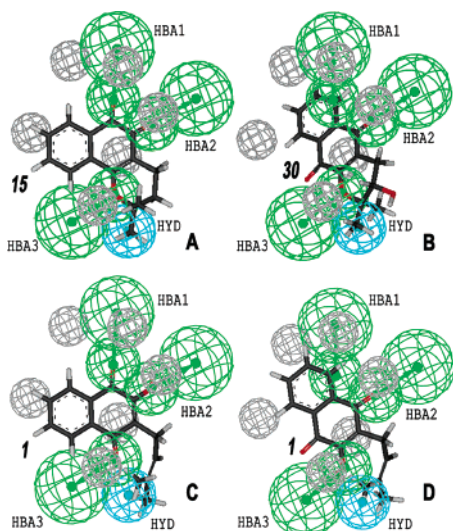
compd	type	$n$	$R, X, Y$	$R_1$	$R_2$	$R_3$	$IC_{50} \pm SD$ (mM)				$\Delta G_{solv}$ (kcal/mol)	$\log P$
							exptl	rank	est Catalyst	est CoMSIA		
<b>39</b>	1	1	$X = NOH$ $Y = O$	Me	Me	H	$3.20 \pm 0.3$	++	2.2	1.5	-9.1	4.6
<b>40</b>	2	0	$X = NO_2$ $Y = OH$	$CH(OH)(CH_3)_2$	H	H	$46.97 (12.0)$	+	54	56	-10.4	2.7
<b>41</b>	3		$-(CH_2)_4-$				$15.53 \pm 1.1$	+	22	18	-8.8	4.2
<b>42</b>	4	1	$-(CH_2)_4-$	Me	Me	H	$\geq 100$	+	20		-8.6	6.4
<b>43</b>	4	1	$-(CH_2)_4-$	Me	Me	OH	$13.39 \pm 5.7$	+	30	19	-12.5	4.8
<b>44</b>	4	1	$-(CH_2)_4-$	Me	Me	OAc	$24.16 \pm 9.2$	+	17	24	-12.1	5.7
<b>45</b>	4	0	$-(CH_2)_4-$	$CH(OH)(CH_3)_2$	H	H	$31.88 (10.9)$	+	25	30 <sup>a</sup>	-10.1	4.2
<b>46</b>	4	1	H	Me	Me	H	$23.68 \pm 7.0$	+	26	30	-8.3	4.7
<b>47</b>	4	1	H	Me	Me	OH	$28.25 \pm 5.3$	+	29	25	-13.1	3.2
<b>48</b>	4	1	H	Me	Me	Br	$24.10 \pm 4.5$	+	28	26	-8.4	4.8
<b>49</b>	4	0	H	$CH(OH)(CH_3)_2$	H	H	$44.08 \pm 9.6$	+	37	40	-13.6	2.5
<b>50</b>	5	1	H	Me	Me	H	$47.10 \pm 7.9$	+	59		-10.6	3.9
<b>51</b>	5	0	H	$CH(OH)(CH_3)_2$	H	H	$g100$	+	37		-14.8	2.4

<sup>a</sup> Compounds used to test the CoMSIA model.

bond-acceptor groups (HBA1, HBA2 and HBA3), and six excluded volumes. The theoretically predicted  $IC_{50}$  values are also listed in Tables 1–4. The good predictive power of this model is indicated by the high correlation coefficient between experimentally and theoretically predicted  $IC_{50}$  values ( $r = 0.937$ ). In fact, only one +++ compound is not correctly predicted in the ++ category (compound **10**); only one ++ compound is incorrectly classified in the + category (compound **10**); and all but four + compounds (**3**, **5**, **36**, and **38**) were predicted correctly. All compounds that are highly active (++++) fit the HYD, HBA1, HBA2, and HBA3 pharmacophoric features with the exception of compound **10**.

**Three-Dimensional QSAR/CoMSIA Model for Naphthoquinone Derivatives.** Three-dimensional QSAR/CoMSIA analysis was performed on naphthoquinones **1–51** (Tables 1–4). Randomly chosen compounds **12**, **20**, **32**, and **45** were not included in the training set in order to test the derived CoMSIA model predictiveness. The inactive compounds **42**, **50**, and **51** were not included in the CoMSIA model, because their residual values were greater than two standard deviations. The experi-

mentally determined  $IC_{50}$  values were related to the independent variables by the PLS methodology (see Experimental Section). Table 5 shows the statistical properties of the model. From a statistical viewpoint, the value of the obtained cross-validated correlation coefficient  $q^2$  (0.627) reveals that the model is a useful tool for predicting the biological activity. The correlation coefficient between theoretically predicted (see Tables 1–4) and experimentally determined  $IC_{50}$  values is 0.933. As a further test of robustness, the CoMSIA model was applied to the excluded ligands **12**, **20**, **32**, and **45**. Clearly the theoretically predicted values for these compounds (marked in Tables 1–4) are in agreement with the experimentally determined ones. The relative contributions of the CoMSIA models for the electrostatic, steric, hydrogen-bond-donor and -acceptor, hydrophobic, and solvation terms are also shown in Table 5. Figure 2 illustrates the CoMSIA (i) steric, (ii) electrostatic, (iii) hydrophobic, (iv) hydrogen-bond-acceptor and (v) hydrogen-bond-donor fields on the receptor maps (the color code of the maps is described in the caption).



**Figure 1.** Pharmacophore model for naphthoquinone derivatives 1–51 created with the HypoGen algorithm as implemented in Catalyst. The structural features are a hydrophobic region (HYD, cyan), three hydrogen-bond-acceptor groups (HBA1, HBA2, and HBA3, green), and six excluded volumes (gray). The HYD feature is drawn as a globe, whereas HBA features are shown as two globes due to the directional nature of this chemical function.  $\beta$ -Cycled-1,2-naphthoquinone **15** (A),  $\alpha$ -cycled-1,4-naphthoquinone **30** (B), and lapachol **1** (C, D) were mapped onto the pharmacophore model.

## Discussion

**Pyran-1,2-Daphthoquinone Derivatives ( $\beta$ -Cycled, Angular Tricyclic Compounds).** All pyran-1,2-naphthoquinones ( $n = 1$ ) are highly active (+++) compounds (see Table 2). These compounds share all the chemical features found in the pharmacophore model. Figure 1A shows compound **15** placed into the model. Clearly, the carbonyl groups at the C-1 (HBA1) and C-2 (HBA2) positions, and the oxygen atom of the pyran ring (HBA3), act as hydrogen-bond acceptors in a hydrogen-bond interaction with the receptor, whereas the HYD feature is created in this selected set of ligands by the methyl groups at the C-13 position of the pyran ring ( $R_1 = R_2 = \text{Me}$ ). The CoMSIA analysis reproduces similar structural determinants (Figure 2A). The electrostatic map (Figure 2A<sub>ii</sub>) and H-bond-donor map (Figure 2A<sub>v</sub>) on the receptor show magenta and orange areas at the upper right side near the carbonyl groups at C-1 and C-2, which are similar to the HBA1 and HBA2 pharmacophoric elements. In agreement with this hypothesis that hydrogen-bond-donor groups at the receptor interact with the two carbonyl groups, the steric map (Figure 2A<sub>i</sub>) shows an unfavorable yellow area at this position where the receptor would be located. The steric map also contains a favorable green area similar to the HYD feature (Figure 2A<sub>i</sub>, lower right side). However, the HBA3 pharmacophoric element is not reproduced in the CoMSIA analysis.

Compound **39** is, among the ligands described in Table 4, the only one showing moderate activity (++). Remarkably, this compound has in common with the pyran-1,2-naphthoquinones the HBA2 carbonyl group, the HBA3 oxygen atom at the pyran ring, and the HYD methyl groups. However, the HBA1 feature in **39** is attained by the oxime  $-\text{C}=\text{NOH}$  group rather than the carbonyl group at the C-1 position of the pyran-1,2-naphthoquinones. The longer  $-\text{C}=\text{NOH}$  group is probably not optimal for interacting with the receptor at this part of the molecule. In contrast to the carbonyl group, the NOH can also act as hydrogen-bond donor. The  $-\text{C}=\text{NOH}$  moiety is predicted in the CoMSIA model to interact with the cyan area at the upper

**Table 5.** Statistical Results of Inhibition of Cell Growth ( $\text{IC}_{50}$ ) in the CoMSIA Model

$Q^2$ <sup>a</sup>	0.627
$N^b$	4
$n^c$	44
$R^2$ <sup>d</sup>	0.933
F	135.162
electrostatic <sup>e</sup>	24.1
steric <sup>e</sup>	7.2
H-bond acceptor <sup>e,f</sup>	17.7
H-bond donor <sup>e,f</sup>	33.6
hydrophobic <sup>e</sup>	15.7
solvation <sup>e</sup>	1.6

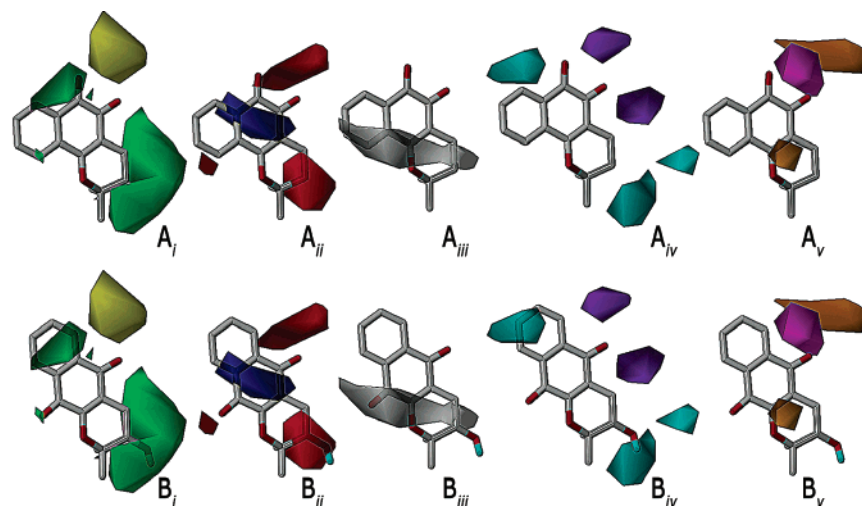
<sup>a</sup> Leave-one-out correlation coefficient. <sup>b</sup> Optimal number of principal components. <sup>c</sup> Number of compounds. <sup>d</sup> Non-cross-validated correlation coefficient. <sup>e</sup> Percentage of contribution. <sup>f</sup> On the receptor.

left side of Figures 2A<sub>iv</sub> and 3, where H-bond-acceptor groups of the receptor are located.

The substitution of  $R_3 = \text{H}$  in **15** [ $\text{IC}_{50}$  (**15**) = 0.27] by polar groups such as OH [ $\text{IC}_{50}$  (**16**) = 0.57 and  $\text{IC}_{50}$  (**17**) = 0.55] or OAc [ $\text{IC}_{50}$  (**23**) = 0.68] increases the  $\text{IC}_{50}$  values; whereas substitution by Br [ $\text{IC}_{50}$  (**19**) = 0.13 and  $\text{IC}_{50}$  (**20**) = 0.20] or by a voluminous and polar group (**27**, **28**) decreases the  $\text{IC}_{50}$  values. This small dependence on the substituent of  $R_3$ , ranging from  $\text{IC}_{50}$  (**28**) = 0.11 to  $\text{IC}_{50}$  (**23**) = 0.68, is not represented in the pharmacophore model and only partially represented in the CoMSIA analysis. Steric (Figure 2A<sub>i</sub>), electrostatic (Figure 2A<sub>ii</sub>), and H-bond acceptor (Figure 2A<sub>iv</sub>) fields on the receptor maps show green, red, and cyan areas, respectively, indicating that the  $R_3$  substitution modulates the  $\text{IC}_{50}$  values. The hydrogen-bond-donor OH group of compounds **16** and **17** would fit the cyan area where H-bond acceptor groups on the receptor should be located; however, the  $\text{IC}_{50}$  increase of compounds **16** and **17** ( $R_3 = \text{OH}$ ) with respect to compound **15** ( $R_3 = \text{H}$ ) is not explained by the CoMSIA model in 1,2-naphthoquinones ( $\beta$ -cycled). In contrast, the OH substitution in 1,4-naphthoquinones ( $\alpha$ -cycled) decreases the  $\text{IC}_{50}$  values in agreement with the CoMSIA model, as will be discussed later. This different behavior of 1,2- and 1,4-naphthoquinones having OH substitutions supports the idea of different orientations in the interaction with the receptor (see next section).

**Pyran- ( $n = 1$ ) and Furan- ( $n = 0$ ) 1,4-Naphthoquinone Derivatives ( $\alpha$ -Cycled, Linear Tricyclic Compounds).** None of the synthesized 1,4-naphthoquinone derivatives shows high cytotoxic activity, despite the fact that they contain chemical features similar to the 1,2-naphthoquinones: that is, two carbonyl moieties, the oxygen atom of the pyran or furan ring, and two methyl groups (see Table 3). However, these common elements show different spatial arrangement in the two types of naphthoquinones. Figure 1B shows superposition of compound **30** into the pharmacophoric model. The carbonyl group at the C-4 position elicits the HBA2 feature, the oxygen atom of the pyran ring elicits the HBA3 feature, and the methyl groups of the pyran ring elicit the HYD feature. In contrast to 1,2-naphthoquinones, the carbonyl group at the C-1 position of 1,4-naphthoquinones is not coordinated with any HBA feature, explaining the fact that this set of compounds is moderately active (++) or inactive (+) (Table 3).

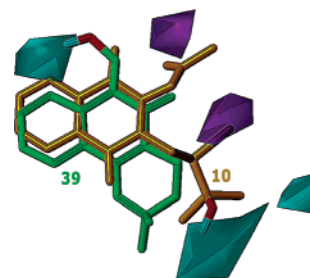
Figure 2B shows compound **30** placed into the CoMSIA model. The hydrogen-bond-donor group  $R_3 = \text{OH}$  is predicted to map to the cyan area (Figure 2B<sub>iv</sub>) where H-bond-acceptor groups of the receptor are located. This fact explains the 10-fold decrease of  $\text{IC}_{50}$  between compounds **36** ( $R_3 = \text{H}$ ) and **30** ( $R_3 = \text{OH}$ ). The same effect is not observed in 1,2-naphthoquinones (see above).



**Figure 2.** Steric (i), electrostatic (ii), hydrophobic (iii), hydrogen-bond-acceptor (iv), and hydrogen-bond-donor (v) maps for the IC<sub>50</sub> CoMSIA model.  $\beta$ -Cycled-1,2-naphthoquinone **15** (A) and  $\alpha$ -cycled-1,4-naphthoquinone **30** (B) are shown as reference structures. The color code of the maps is as follows: (i) green or yellow areas depict zones of the space where occupancy by the ligands decreases or increases IC<sub>50</sub>, respectively; (ii) areas where a high electron density provided by the ligand decreases or increases IC<sub>50</sub> are shown in red or blue, respectively; (iii) gray areas define regions of space where hydrophobic groups are predicted to increase IC<sub>50</sub>; (iv) areas where H-bond acceptors on the receptor are predicted to decrease or increase IC<sub>50</sub> are shown in cyan or purple, respectively; and (v) orange or magenta contours show areas where H-bond donor zones on the receptor are predicted to increase or decrease IC<sub>50</sub>.

#### 1,4-Naphthoquinone Derivatives (Bicyclic Compounds).

1,4-Naphthoquinone derivatives (Table 1) contain two carbonyl moieties, at positions similar to the carbonyls of the  $\alpha$ -cycled 1,4-naphthoquinones, and an oxygenated substituent at C-2, comparable to the oxygen atom of the pyran or furan ring of  $\alpha$ -cycled 1,4-naphthoquinones. The tricyclic 1,4-naphthoquinones ( $\alpha$ -cycled) are more rigid structures than the corresponding bicyclic 1,4-naphthoquinones (opened), in which the R<sub>1</sub> and R<sub>2</sub> substituents can adopt different conformations and, consequently, achieve different binding modes into the pharmacophore model. This effect is illustrated in Figure 1C,D for lapachol **1**. Figure 1D shows superposition of lapachol into the pharmacophoric model through the C-4 carbonyl group in HBA2, the R<sub>1</sub> = OH substituent at C-2 in HBA3, and the isoprenyl chain in HYD. Notably, the aliphatic chain at C-3 adopts the same conformation as the pyran ring of  $\alpha$ -cycled 1,4-naphthoquinones. This mode of binding is, thus, similar to  $\alpha$ -cycled 1,4-naphthoquinones (see Figure 1B,D), and it would explain the moderately active (++) or inactive (+) profile of this set of compounds (Table 1). Figure 1C shows the other arrangement of lapachol **1** into the pharmacophore model. In this case, the C-1 carbonyl group, the hydroxyl group at C-2, and the carbonyl group at C-4 act as hydrogen-bond acceptors mapping HBA1, HBA2, and HBA3, respectively, whereas the aliphatic chain at R<sub>2</sub> maps the HYD. However, the bicyclic 1,4-naphthoquinones possess moderate activity or inactivity, in contrast with the high cytotoxicity of  $\beta$ -cycled 1,2-naphthoquinones [IC<sub>50</sub> (**1**) = 3.18 vs IC<sub>50</sub> (**15**) = 0.27]. This different behavior can be explained by considering that the HYD methyl groups of **15** are forced by the pyran ring to keep their spatial arrangement (see above), whereas the aliphatic chain of **1** probably changes conformation to be placed at the HYD feature, causing an energetic penalty. The electronic nature of the C-2 carbonyl oxygen of **15** and the OH substituent of **1** is very different. Both functional groups map the HBA2 feature but in a different way. While the carbon and oxygen atoms and the lone pairs of C=O are in the same plane in **15**, the carbon, oxygen, and hydrogen atoms and the lone pairs of the OH group are in a tetrahedral arrangement in **1**. Thus, the OH group of **1** cannot have a hydrogen-bond interaction of the same magnitude as the C=O group of **15**.



**Figure 3.** Hydrogen-bond acceptor on the receptor map for the IC<sub>50</sub> CoMSIA model with compounds **10** (yellow) and **39** (green) shown as reference structures. The color code for the contour maps is as described for Figure 2.

The replacement of the double bond of the isoprenyl chain [IC<sub>50</sub> (**2**) = 4.51] by other groups has varied effects on the cytotoxicity. Compound **10**, with R<sub>2</sub> = CH<sub>2</sub>CHBrC(OH)(CH<sub>3</sub>)<sub>2</sub>, presents a cytotoxic activity increase of 8.7-fold with respect to compound **2** [IC<sub>50</sub> (**10**) = 0.52]. Figure 3 shows this compound in orange into the hydrogen-bond-acceptor map of the CoMSIA model. Clearly, the OH group maps the cyan area at the lower right side of the figure, where H-bond-acceptor groups at the receptor are located, explaining the significant decrease in IC<sub>50</sub> of this compound. The CoMSIA model also predicts an unfavorable purple area, which explains the inactivity of **9** [IC<sub>50</sub> (**9**) = 48.1], which presents two hydroxyl groups on the isoprenyl chain [R<sub>2</sub> = CH<sub>2</sub>CH(OH)C(OH)(CH<sub>3</sub>)<sub>2</sub>]. The hydroxyl group at C-2 maps onto this unfavorable area.

**Nitrogenous Derivatives.** The nitrogenous derivatives (**40**–**51**, Table 4) are inactive compounds. Clearly, compounds **41**–**51** occupy the yellow contour area in the steric map of Figure 1, near the C-1 and C-2 carbons, showing that occupancy of this area by the heterocyclic ring of these compounds is detrimental for cytotoxic activity.

#### Conclusions

In conclusion, our study has identified in detail the structural elements of naphthoquinone derivatives that are keys for cytotoxic activity in the HL-60 cell line. The independent generation of a HypoGen pharmacophore model and a 3D-



QSAR/CoMSIA model, using the alignment obtained with the former, has been shown to be a valuable tool for analysis. Highly active compounds, such as  $\beta$ -cycled pyran-1,2-naphthoquinones [ $0.1 \mu\text{M} < \text{IC}_{50} < 0.57 \mu\text{M}$ ], contain four pharmacophoric features: three hydrogen-bond-acceptor groups and a hydrophobic region. These results provide the tools for the design and synthesis of new ligands with high predetermined activities.

## Experimental Section

**General.** IR spectra were obtained on a Bruker IFS 55 spectrophotometer. One-dimensional (1D) NMR spectra ( $^1\text{H}$  and  $^{13}\text{C}$  NMR) were recorded on a Bruker AMX-300 spectrometer. Two-dimensional NMR spectra were registered on Bruker AMX-400 spectrometer. Chemical shifts ( $\delta$ ) are expressed in parts per million (ppm), and coupling constants ( $J$ ) are given in hertz. Mass spectra [electron ionization mass spectrometry (EI-MS) and high-resolution (HR) EI-MS] were analyzed on Micromass Autospec. TLC 1500/LS 25 Schleicher and Schuell foils were used for thin-layer chromatography, while silica gel (0.2–0.63 mm) and Sephadex LH-20 were used for column chromatography. Lapachol **1**,  $\beta$ -lapachone **15**, and lawsone **53** were used as starting material to synthesize the training set of naphthoquinones. Lapachol **1** was isolated by extraction of the powdered wood of *Tabebuia impetiginosa* (Bignoniaceae) with a cold solution of sodium carbonate 1%.  $\beta$ -Lapachone **15** was obtained by intramolecular cyclization of lapachol using concentrated sulfuric acid.<sup>7c</sup> Lawsone **53** (2-hydroxy-1,4-naphthoquinone) was purchased from Sigma–Aldrich Co. Compounds **2–10**, **16–18**, and **30–51** were obtained following the same procedure described in refs 3, 5b, 7c, 21, and 23. Compounds **19–23** were obtained in higher yield than previously reported methods by following the procedure described below. The procedures for the preparation of derivatives **11–14** and **23–29** are also described below. Spectroscopic data of the new compounds **11**, **14** and **24–29**, whose structures were rigorously elucidated and have not been previously reported in the literature, are also included.

**3-(2,3-Dibromo-3-methylbutyl)-1,4-dioxo-1,4-dihydro-2-naphthalenyl Acetate (11).** Compound **2** (262 mg) was treated with 1.1 equiv of NBS in  $^t\text{BuOH}/\text{H}_2\text{O}$  (1/1). When the starting material was consumed, the solvent was removed to half of its volume, the crude material was extracted with ether, and the combined organic extracts were dried over  $\text{MgSO}_4$ . The mixture was purified on a Sephadex LH-20 column (eluted with a mixture of hexanes/MeOH/ $\text{CHCl}_3$  2/1/1) to yield 330 mg (94%) of **10** and 11 mg (3%) of **11**. Compound **10** showed spectroscopic data in agreement with those reported previously in the literature.  $^1\text{H}$  NMR ( $\text{CDCl}_3$ , 300 MHz)  $\delta$  8.12 (m, 2H), 7.76 (m, 2H), 3.60 (dd,  $J = 10.1$ , 2.6 Hz, 1H), 3.04 (dd,  $J = 12.9$ , 2.7 Hz, 1H), 2.81 (dd,  $J = 12.9$ , 10.1 Hz, 1H), 2.41 (s, 3H), 1.86 (s, 3H), 1.85 (s, 3H).  $^{13}\text{C}$  NMR ( $\text{CDCl}_3$ , 75 MHz)  $\delta$  185.4 (s), 177.8 (s), 168.1 (s), 152.5 (s), 136.5 (s), 134.2 (d), 134.1 (d), 131.9 (s), 130.9 (s), 126.8  $\times$  2 (d), 77.8 (d), 73.1 (s), 30.4 (t), 30.0 (q), 28.6 (q), 20.5 (q). EI-MS  $m/z$  444 ( $\text{M}^+ + 2$ , 27), 442 ( $\text{M}^+$ , 70), 361 ( $\text{M}^+ - \text{Br}$ , 58), 154 (100). HR-EI-MS  $m/z$  441.9409 [ $\text{M}^+$ ]; calcd for  $\text{C}_{17}\text{H}_{16}\text{O}_4\text{Br}_2$  441.9415]. IR ( $\text{CHCl}_3$ )  $\nu_{\text{max}}$  ( $\text{cm}^{-1}$ ) 3527, 2970, 1777, 1677, 1595, 1430, 1370, 1340, 1296, 1173, 1068, 1015, 947, 878, 793, 733  $\text{cm}^{-1}$ .

**Hydrogenation of Lapachol (1) To Obtain Derivatives 12 and 13.** Compound **1** (183 mg) was dissolved in 10 mL of dry tetrahydrofuran (THF). Catalytic amounts of Pd supported on carbon were added and a stream of  $\text{H}_2$  was passed through the mixture for 10 days. Then the crude product was filtered and the solvent was eliminated under vacuum. The residue was chromatographed by preparative TLC (eluted with a mixture of hexanes/acetate 10%), yielding 50 mg (27%) of **12** and 94 mg (51%) of **13**. Both showed spectroscopic data identical to those reported previously in the literature.<sup>26</sup>

**2-Isopentyl-3-(methoxymethoxy)naphthoquinone (14).** Compound **13** (40 mg) was treated with 1.6 equiv of methoxymethylchloride (MOMCl) and 2 equiv of ethylisopropylamine ( $^i\text{Pr}_2\text{EtN}$ ) in 4 mL of dry  $\text{CH}_2\text{Cl}_2$  at room temperature (rt) for 30 min. The mixture was washed with  $\text{H}_2\text{O}$  and the combined organic phases

were dried over  $\text{MgSO}_4$ . After evaporation of the solvent, the residue was chromatographed on a Sephadex LH-20 column (eluted with a mixture of hexanes/MeOH/ $\text{CHCl}_3$  2/1/1), yielding 47 mg (100%) of **14**.  $^1\text{H}$  NMR ( $\text{CDCl}_3$ , 300 MHz)  $\delta$  8.05 (m, 2H), 7.69 (m, 2H), 5.43 (s, 2H), 3.57 (s, 3H), 2.64 (m, 2H), 1.63 (hept,  $J = 6.6$  Hz, 1H), 1.39 (m, 2H), 0.96 (d,  $J = 6.6$  Hz, 6H).  $^{13}\text{C}$  NMR ( $\text{CDCl}_3$ , 75 MHz)  $\delta$  185.2 (s), 181.4 (s), 155.3 (s), 137.3 (s), 133.8 (d), 133.2 (d), 132.0 (s), 131.3 (s), 126.2  $\times$  2 (d), 98.4 (t), 57.6 (q), 37.8 (t), 28.6 (d), 22.4  $\times$  2 (q), 22.1 (t). EI-MS  $m/z$  288 ( $\text{M}^+$ , 0.5), 257 ( $\text{M}^+ - \text{OMe}$ , 0.4), 244 ( $\text{M}^+ - \text{MOM}$ , 37), 188 (100). HR-EI-MS  $m/z$  288.1371 [ $\text{M}^+$ ]; calcd for  $\text{C}_{17}\text{H}_{20}\text{O}_4$  288.1362].

**Reaction of 1 with NBS To Obtain Derivatives 19, 20, 22, and 31.** Compound **1** (2.25 g) was treated with 2 equiv of NBS in  $\text{CH}_2\text{Cl}_2$  for 24 h. Then the solvent was removed under vacuum and the residue was purified by flash chromatography on silica gel, eluted with hexanes/EtOAc 3/2, to yield 875 mg (29%) of **19**, 752 mg (25%) of 12-bromo- $\beta$ -dehydrolapachone **20**, 773 mg (25%) of **22**, 51 mg (2%) of **31**, and 6 mg (<1%) of the 12-bromo- $\alpha$ -dehydrolapachone isomer. All of them showed spectroscopic data identical to those reported previously in the literature.<sup>27</sup>

**Reaction of 2 with  $\text{Br}_2$  To Obtain Derivatives 19 and 21.** Compound **2** (184 mg, 0.65 mmol) was treated with 1.0 equiv of  $\text{Br}_2$  in 10 mL of dry  $\text{CH}_2\text{Cl}_2$  at rt for 10 min. The solvent was removed under vacuum and the crude product was purified by flash chromatography (eluted with hexanes/EtOAc 40%) to yield 171 mg of compound **19** (93%) and 11 mg of compound **21** (5%), which showed spectroscopic data identical to those reported.<sup>27</sup>

**General Procedure for Preparation of the ( $\pm$ ) Ester Derivatives 23–27.** The racemic alcohol **52** was treated with 1.5 equiv of the corresponding acyl chloride and 2 equiv of pyridine, in dry  $\text{CH}_2\text{Cl}_2$  at 0  $^\circ\text{C}$ . When the starting material was consumed (as monitored by TLC), the reaction mixture was left to warm to rt, the solvent was removed under reduced pressure, and the crude product was chromatographed on silica gel with mixtures of hexane/EtOAc as eluent. Compound **23** showed spectroscopic data identical to those reported previously in the literature.<sup>28</sup>

**( $\pm$ )-2,2-Dimethyl-5,6-dioxo-3,4,5,6-tetrahydro-2H-benzo[h]-chromen-3-yl 2-Methylpropanoate (24).** Following the procedure described above, 103 mg (0.39 mmol) of ( $\pm$ )-**52** was treated with 65  $\mu\text{L}$  (1.5 equiv) of isobutyryl chloride and 65  $\mu\text{L}$  (2 equiv) of pyridine, in 6 mL of  $\text{CH}_2\text{Cl}_2$  at 0  $^\circ\text{C}$  for 18 h. The crude was purified by flash chromatography with 5–20% hexanes/EtOAc, to yield 129 mg (100%) of **24**.  $^1\text{H}$  NMR ( $\text{CDCl}_3$ , 300 MHz)  $\delta$  8.08 (d,  $J = 7.6$  Hz, 1H), 7.83 (d,  $J = 7.8$  Hz, 1H), 7.67 (t,  $J = 7.7$  Hz, 1H), 7.54 (t,  $J = 7.7$  Hz, 1H), 5.12 (t,  $J = 4.8$  Hz, 1H), 2.83 (dd,  $J = 18.1$ , 5.0 Hz, 1H), 2.63 (dd,  $J = 18.1$ , 4.6 Hz, 1H), 2.54 (qq,  $J = 7.0$ , 7.0 Hz, 1H), 1.47 (s, 3H), 1.44 (s, 3H), 1.47 (t,  $J = 7.0$  Hz, 6H).  $^{13}\text{C}$  NMR ( $\text{CDCl}_3$ , 75 MHz)  $\delta$  179.3 (s), 178.5 (s), 176.0 (s), 161.1 (s), 134.9 (d), 131.9 (s), 131.0 (d), 130.1 (s), 128.8 (d), 124.7 (d), 110.2 (s), 79.8 (d), 68.8 (d), 34.0 (d), 25.0 (q), 22.9 (q), 22.6 (t), 19.0 (q), 18.8 (q). EI-MS  $m/z$  329 ( $\text{M}^+ - 2$ ), 258 ( $\text{M}^+ - \text{COPri}$ , 2), 258 ( $\text{M}^+ - \text{COPri} - \text{H}_2\text{O}$ , 100), 212 (240 - CO, 60), 71 ( $\text{COPri}$ , 46). HR-EI-MS  $m/z$  329.1401 [ $\text{M}^+ + 1$ ]; calcd for  $\text{C}_{19}\text{H}_{21}\text{O}_5$  329.1389].

**( $\pm$ )-2,2-Dimethyl-5,6-dioxo-3,4,5,6-tetrahydro-2H-benzo[h]-chromen-3-yl Laurate (25).** Following the general procedure described above, 140 mg (0.54 mmol) of ( $\pm$ )-**52** was treated with 190  $\mu\text{L}$  (1.5 equiv) of lauroyl chloride and 90  $\mu\text{L}$  (2 equiv) of pyridine, in 8 mL of  $\text{CH}_2\text{Cl}_2$  at 0  $^\circ\text{C}$  for 6 h. The crude product was purified by flash chromatography, eluted with hexanes/EtOAc 9/1, to yield 208 mg (87%) of **25**.  $^1\text{H}$  NMR ( $\text{CDCl}_3$ , 300 MHz)  $\delta$  8.03 (d,  $J = 7.6$  Hz, 1H), 7.81 (d,  $J = 7.8$  Hz, 1H), 7.64 (t,  $J = 7.7$  Hz, 1H), 7.50 (t,  $J = 7.6$  Hz, 1H), 5.11 (m, 1H), 2.78 (dd,  $J = 18.2$ , 4.9 Hz, 1H), 2.63 (dd,  $J = 18.2$ , 4.3 Hz, 1H), 2.30 (m, 6H), 1.56 (m, 6H), 1.45 (s, 3H), 1.41 (s, 3H), 0.83 (m, 11H).  $^{13}\text{C}$  NMR ( $\text{CDCl}_3$ , 75 MHz)  $\delta$  179.2 (s), 178.4 (s), 162.1 (s), 134.8 (d), 131.9 (s), 130.9 (d), 130.1 (s), 128.7 (d), 124.2 (d), 110.1 (s), 79.7 (s), 68.8 (d), 34.2 (t), 34.0 (t), 31.8 (t), 29.5 (t), 29.4 (t), 29.3 (t), 29.2 (t), 29.1 (t), 29.0 (t), 24.9 (s), 24.8 (q), 24.7 (t), 23.0 (t), 22.6 (q), 14.0 (q). EI-MS  $m/z$  440 ( $\text{M}^+$ , 7), 240 [ $\text{M}^+ - \text{OCO}(\text{CH}_2)_{10}\text{CH}_3$ , 100]. HR-EI-MS  $m/z$  440.2542 [ $\text{M}^+$ ]; calcd for  $\text{C}_{27}\text{H}_{36}\text{O}_5$  440.2563].

( $\pm$ )-2,2-Dimethyl-5,6-dioxo-3,4,5,6-tetrahydro-2H-benzo[h]-chromen-3-yl 4-Bromobenzoate (**26**). ( $\pm$ )-**52** (133 mg, 0.51 mmol) was treated with 170 mg (1.5 equiv) of *p*-bromobenzoyl chloride and 80  $\mu$ L (2 equiv) of pyridine, in 15 mL of  $\text{CH}_2\text{Cl}_2$  at 0 °C. The crude product was purified by flash chromatography, eluted with hexanes/EtOAc 9/1, to yield 12 mg (5%) of **26**.  $^1\text{H}$  NMR ( $\text{CDCl}_3$ , 300 MHz)  $\delta$  8.03 (m, 2H), 7.99 (d,  $J$  = 7.8 Hz, 2H), 7.83 (d,  $J$  = 7.8 Hz, 1H), 7.68 (m, 2H), 7.50 (m, 1H), 5.40 (m, 1H), 2.95 (dd,  $J$  = 18.3, 4.7 Hz, 1H), 2.85 (dd,  $J$  = 18.3, 4.0 Hz, 1H), 1.55 (s, 3H), 1.52 (s, 3H).  $^{13}\text{C}$  NMR ( $\text{CDCl}_3$ , 75 MHz)  $\delta$  179.3 (s), 178.2 (s), 163.1 (s), 150.9 (s), 134.1 (d), 132.2  $\times$  2 (d), 132.1 (s), 131.9  $\times$  2 (d), 130.1 (s), 129.0 (d), 125.9 (d), 124.3 (d), 127.7 (s), 127.0 (s), 109.8 (s), 79.1 (s), 70.6 (d), 24.9 (q), 23.5 (q), 22.7 (t). EI-MS  $m/z$  442 ( $\text{M}^+$  + 2, 8), 440 ( $\text{M}^+$ , 8), 257 [ $\text{M}^+$  -  $\text{COP}(\text{Br})\text{Ph}$ , 61], 183 [ $\text{COP}(\text{Br})\text{Ph}$ , 100]. HR-EI-MS  $m/z$  440.0278 [ $\text{M}^+$ ]; calcd for  $\text{C}_{22}\text{H}_{17}\text{O}_5\text{Br}$  440.0310].

( $\pm$ )-2,2-Dimethyl-5,6-dioxo-3,4,5,6-tetrahydro-2H-benzo[h]-chromen-3-yl 4-Cyanobenzoate (**27**). ( $\pm$ )-**52** (130 mg, 0.50 mmol) in 10 mL of  $\text{CH}_2\text{Cl}_2$  was treated with 170 mg (2 equiv) of *p*-cyanobenzoyl chloride and 100  $\mu$ L (2.5 equiv) of pyridine, at 0 °C for 24 h. The crude product was purified by flash chromatography, with 5–40% hexanes/EtOAc, to yield 51 mg (35%) of **27**.  $^1\text{H}$  NMR ( $\text{CDCl}_3$ , 300 MHz)  $\delta$  8.11 (d,  $J$  = 7.6 Hz, 1H), 8.06 (d,  $J$  = 7.7 Hz, 2H), 7.89 (d,  $J$  = 7.6 Hz, 1H), 7.68 (m, 3H), 7.58 (m, 1H), 5.40 (m, 1H), 2.95 (dd,  $J$  = 18.4, 4.8 Hz, 1H), 2.85 (dd,  $J$  = 18.4, 4.0 Hz, 1H), 1.57 (s, 3H), 1.51 (s, 3H).  $^{13}\text{C}$  NMR ( $\text{CDCl}_3$ , 75 MHz)  $\delta$  179.1 (s), 178.5 (s), 163.9 (s), 161.1 (s), 135.0 (d), 133.2 (s), 132.3  $\times$  2 (d), 131.8 (s), 131.2 (d), 130.6 (s), 130.2  $\times$  2 (d), 129.0 (d), 124.3 (d), 117.7 (s), 116.9 (s), 109.8 (s), 79.1 (s), 70.6 (d), 24.9 (q), 23.5 (q), 22.7 (t). EI-MS  $m/z$  387 ( $\text{M}^+$ , 1), 258 [ $\text{M}^+$  -  $\text{COP}(\text{CN})\text{Ph}$ , 1], 130 [ $\text{COP}(\text{CN})\text{Ph}$ , 94 (100)]. HR-EI-MS  $m/z$  387.3401 [ $\text{M}^+$ ]; calcd for  $\text{C}_{23}\text{H}_{17}\text{O}_5\text{N}$  387.3854].

**Resolution of 3-Hydroxy-2,2-dimethyl-3,4-dihydro-2H-benzo[h]-chromene-5,6-dione (**52**): Preparation of Esters **28** and **29**.** ( $\pm$ )-**52** (149 mg, 0.58 mmol) in 6 mL of dry  $\text{CH}_2\text{Cl}_2$  was treated with 192 mg (2 equiv) of (*R*)- $\alpha$ -methoxyphenylacetic acid, at rt for 10 h in the presence of dicyclohexylcarbodiimide (2 equiv) and dimethylaminopyridine (DMAP) in catalytic amounts. When the starting material was consumed, the solvent was removed under vacuum and the crude product was purified by flash chromatography (silica gel, eluted with mixtures of hexanes/EtOAc increasing the polarity from 5% to 40%) to yield 105 mg (45%) of the *RS* diastereomer **28** and 117 mg (50%) of the *RR* diastereomer **29**. Both esters were hydrolyzed with  $\text{NaHCO}_3$  (0.1 M) in methanol at rt, to yield enantiomeric alcohols **16** and **17** in 36% and 58% yield, respectively.

(*3S*)-2,2-Dimethyl-5,6-dioxo-3,4,5,6-tetrahydro-2H-benzo[h]-chromen-3-yl (*2R*)-Methoxy(phenyl)ethanoate (**28**).  $[\alpha]_{\text{D}}^{25}$  ( $\text{CHCl}_3$ ) = -7.  $^1\text{H}$  NMR ( $\text{CDCl}_3$ , 300 MHz)  $\delta$  8.08 (d,  $J$  = 7.6 Hz, 1H), 7.76 (d,  $J$  = 7.7 Hz, 1H), 7.67 (t,  $J$  = 7.6 Hz, 1H), 7.55 (t,  $J$  = 7.7 Hz, 1H), 7.37 (m, 2H), 7.28 (m, 3H), 5.10 (t,  $J$  = 4.2 Hz, 1H), 4.74 (s, 1H), 3.40 (s, 3H), 2.82 (dd,  $J$  = 18.1, 4.9 Hz, 1H), 2.67 (dd,  $J$  = 18.1, 4.7 Hz, 1H), 1.22 (s, 3H), 1.06 (s, 3H).  $^{13}\text{C}$  NMR ( $\text{CDCl}_3$ , 75 MHz)  $\delta$  179.2 (s), 178.4 (s), 169.6 (s), 161.0 (s), 136.0 (s), 134.8 (d), 131.9 (s), 131.0 (d), 130.1 (s), 128.9 (d), 128.8 (d), 128.6  $\times$  2 (d), 126.8  $\times$  2 (d), 124.2 (d), 109.8 (s), 82.3 (d), 79.6 (s), 69.8 (d), 57.4 (q), 24.7 (q), 22.6 (t), 22.3 (q). EI-MS  $m/z$  240 ( $\text{M}^+$  - MPA, 28), 225 (240 - Me, 9), 121 (MPA -  $\text{CO}_2$ , 100). IR ( $\text{CHCl}_3$ )  $\nu_{\text{max}}$  ( $\text{cm}^{-1}$ ): 2924, 2853, 1752, 1654, 1608, 1573, 1455, 1395, 1114, 1027, 754.

(*3R*)-2,2-Dimethyl-5,6-dioxo-3,4,5,6-tetrahydro-2H-benzo[h]-chromen-3-yl (*2R*)-Methoxy(phenyl)ethanoate (**29**).  $[\alpha]_{\text{D}}^{25}$  ( $\text{CHCl}_3$ ) = -412.  $^1\text{H}$  NMR ( $\text{CDCl}_3$ , 300 MHz)  $\delta$  8.05 (d,  $J$  = 7.6 Hz, 1H), 7.78 (d,  $J$  = 7.7 Hz, 1H), 7.66 (t,  $J$  = 7.6 Hz, 1H), 7.55 (t,  $J$  = 7.7 Hz, 1H), 7.24 (m, 2H), 7.09 (m, 3H), 5.04 (t,  $J$  = 4.2 Hz, 1H), 4.73 (s, 1H), 3.38 (s, 3H), 2.57 (dd,  $J$  = 18.3, 4.5 Hz, 1H), 2.41 (dd,  $J$  = 18.3, 3.9 Hz, 1H), 1.46 (s, 3H), 1.34 (s, 3H).  $^{13}\text{C}$  NMR ( $\text{CDCl}_3$ , 75 MHz)  $\delta$  179.2 (s), 178.4 (s), 169.6 (s), 161.0 (s), 136.0 (s), 134.8 (d), 131.9 (s), 131.0 (d), 130.1 (s), 128.9 (d), 128.8 (d), 128.6  $\times$  2 (d), 127.2  $\times$  2 (d), 124.2 (d), 109.8 (s), 82.3 (d), 79.6

(s), 69.8 (d), 57.4 (q), 24.7 (q), 22.6 (t), 22.3 (q). HR-EI-MS  $m/z$  407.1501 [ $\text{M}^+$  + 1]; calcd for  $\text{C}_{24}\text{H}_{23}\text{O}_6$  407.1495].

(*3S*)-3-Hydroxy-2,2-dimethyl-3,4-dihydro-2H-benzo[h]-chromene-5,6-dione (**16**). Hydrolysis of **28** was carried out with  $\text{NaHCO}_3$  (0.1 M) in methanol at rt for 2 h. The residue was extracted several times with  $\text{CH}_2\text{Cl}_2$ . The combined organic extracts were washed with water, dried over  $\text{MgSO}_4$  and then purified by flash chromatography on silica gel (eluted with mixtures of hexanes/AcOEt 30%), to yield 13 mg (36%) of **16** ( $[\alpha]_{\text{D}}^{25}$  ( $\text{CHCl}_3$ ) = +47.2) which showed spectroscopic data identical to those reported in the literature.

(*3R*)-3-Hydroxy-2,2-dimethyl-3,4-dihydro-2H-benzo[h]-chromene-5,6-dione (**17**). Hydrolysis of **29** was carried out following the procedure described before to obtain 21 mg (58%) of **17**, which showed spectroscopic data identical to those for **16** except the optical rotation ( $[\alpha]_{\text{D}}^{25}$  ( $\text{CHCl}_3$ ) = -49.0).

**Cell Culture.** The human promyelocytic leukemia HL-60 cell line established by Gallagher et al.<sup>29</sup> was cultured in suspension in RPMI-1640 medium (Invitrogen) supplemented with 10% heat-inactivated fetal bovine serum, penicillin (10 000 units/mL), and streptomycin in a humidified atmosphere of 95% air and 5%  $\text{CO}_2$  at 37 °C. Cells were maintained at a density  $< 1 \times 10^6$  cells/mL. Cells were resuspended in fresh medium 24 h before each treatment to ensure exponential growth. Stock solutions (100 or 50 mM) of lapachol derivatives were made in dimethyl sulfoxide (DMSO), aliquoted, and stored at -80 °C. Further dilutions were made in culture medium prior to use. In all experiments, the final concentration of DMSO did not exceed 0.5%, a concentration that is not toxic to the cells.

**Assay for Cytotoxicity.** Cytotoxic assays were performed by the MTT procedure.<sup>30</sup> Cells ( $1 \times 10^4$ /well) were exposed to different concentrations of the compounds in 96-well plates for 72 h at 37 °C. Controls and samples were always treated with the same concentrations of vehicle (DMSO). Surviving cells were detected on the basis of their ability to metabolize 3-[4,5-dimethylthiazol-2-yl]-2,5-diphenyltetrazolium bromide (MTT) into formazan crystals. Optical density at 560 nm was used as a measure of cell viability. The MTT dye reduction assay measures mitochondrial respiratory function and can detect earlier than dye-exclusion methods. Cell survival (%) = (mean absorbance in treated wells/mean absorbance in control wells)  $\times$  100. Concentrations inducing 50% inhibition of cell growth ( $\text{IC}_{50}$ ) were determined graphically for each experiment by use of the curve-fitting routine of Prism 2.0 (GraphPad) and the equation derived by De Lean et al.<sup>31</sup>

**Pharmacophore Model.** The pharmacophore model was generated with the HypoGen module of Catalyst 4.10. Compounds **1–51** were built de novo with standard options within the 2D/3D editor sketcher of the program. In cases where the chirality of the active form was not known, all possible stereoisomers were generated and considered. The BEST conformational analysis procedure was applied. The number of conformers was limited to a maximum of 250, with a 20 kcal/mol energy threshold above the calculated global minimum. The experimentally determined  $\text{IC}_{50}$  values of compounds **1–51** span about 2–3 orders of magnitude from  $\text{IC}_{50}$  (**7**) = 68.2  $\mu\text{M}$  to  $\text{IC}_{50}$  (**28**) = 0.1  $\mu\text{M}$ . Therefore, the inactivity spread, uncertainty, and spacing parameters were changed from the default value of 3.0 to 1.5, 1.6, and 1.8, respectively, as proposed by Accelrys for training sets with narrower activity span than usual. The hydrogen-bond-acceptor (HBA) and -donor (HBD), hydrophobic (HYD), and aromatic ring (AR) chemical features were considered for hypothesis generation and up to 10 excluded volumes. Hypothesis selection was done by a cost analysis procedure (represented in bit units) based on three terms: weight cost (increases in a Gaussian form as the feature weight deviates from an idealized value of 2.0); error cost (penalizes the deviation between the estimated activities of the training set and their experimentally determined values); and configuration cost (penalizes the complexity of the hypothesis, should not exceed a maximum value of 18). The error cost contributes the most in determining the overall cost of a hypothesis. In addition, the costs of the ideal hypothesis, the simplest possible hypothesis that fits the data with



minimal cost (fixed cost), and the null hypothesis in which the error cost is high (null cost) are computed by the HypoGen module. These fixed and null costs represent the minimum and maximum energy cost values, respectively. Statistically significant hypotheses possess total costs close to the fixed cost and far away from the null cost values.<sup>32</sup>

**Three-Dimensional QSAR/CoMSIA Model.** A critical step in CoMSIA is to select a proper alignment rule. Naphthoquinone analogues were oriented in space by aligning each compound to the pharmacophoric hypothesis obtained with the Catalyst software (see above). The QSAR table consists of IC<sub>50</sub> as dependent variable and the electrostatic, steric, hydrophobic, hydrogen-donor, and hydrogen-acceptor fields and solvation energy as independent variables. The atom-centered atomic charges used in CoMSIA to evaluate the electrostatic contributions were computed from the molecular electrostatic potential<sup>33</sup> by use of the 6-31G\* basis set. Solvation free energies ( $\Delta G_{\text{solv}}$ ) of **1–51** were calculated with the PM3–SR5.42R procedure within the AMSOL 6.7.2 program.<sup>34</sup> The potential fields were calculated at each lattice intersection of a regularly spaced grid of 2 Å. An sp<sup>3</sup> carbon atom with a van der Waals radius of 1.52 Å carrying a charge of +1.0 served as a probe atom to calculate the fields with an attenuation factor of 0.3.<sup>35</sup> Partial least-squares (PLS) analysis<sup>36</sup> was used to derive linear equations from the resulting matrices. Leave-one-out (LOO) cross-validation was employed to select the number of principal components and to calculate the cross-validated statistics. The final CoMSIA model was generated with non-cross-validation and the number of components suggested by the LOO validation run. The 3D-QSAR/CoMSIA study was carried out with the QSAR module of the SYBYL 7.0 program<sup>37</sup> with default parameters.

**Acknowledgment.** This work was supported by MCYT (SAF2003-04200-CO2-02), CICYT (SAF2004-07103-CO2-02), and Generalitat de Catalunya (SGR2005-00390). E.P.-S. thanks Gobierno Autónomo de Canarias for the short-stay fellowship and ICIC for the postdoctoral fellowship.

## References

- (1) WHO Cancer, [http://www.who.int/hpr/NPH/docs/gs\\_cancer.pdf](http://www.who.int/hpr/NPH/docs/gs_cancer.pdf), <http://www.who.int/dietphysicalactivity/publications/facts/cancer/en/>.
- (2) (a) Driscoll, J. S.; Hazard, G. F.; Wood, H. B.; Goldin, A. Structure–antitumor activity relationships among quinone derivatives. *Cancer Chemother. Rep. Part 2* **1974**, *4*, 1–362. (b) Liu, K. C.; Li, J.; Sakya, S. Synthetic approaches to the 2003 new drugs. *Mini-Rev. Med. Chem.* **2004**, *4*, 1105–1125.
- (3) Ravelo, A.; Estévez-Braun, A.; Chávez, H.; Pérez-Sacau, E.; Mesa-Siverio, D. Recent studies on natural products as anticancer agents. *Curr. Top. Med. Chem.* **2004**, *4*, 241–65.
- (4) Guiraud, P.; Steiman, R.; Campos-Takaki, G. M.; Seigle-Murandi, F.; Simeon de Buochberg, M. S. Comparison of antibacterial and antifungal activities of lapachol and  $\beta$ -lapachone. *Planta Med.* **1994**, *60*, 373–374.
- (5) (a) de Andrade-Neto, V. F.; Goulart, M. O. F.; da Silva Filho, J. F.; da Silva, M. J.; Pinto, M. C. F. R.; Pinto, A. V.; Zalis, M. G.; Carvalhal, L. H.; Krettli, A. U. Antimalarial activity of phenazines from lapachol,  $\beta$ -lapachone and its derivatives against *Plasmodium falciparum* in vitro and *Plasmodium berghei* in vivo. *Bioorg. Med. Chem. Lett.* **2004**, *14*, 1145–49. (b) Pérez-Sacau, E.; Estévez-Braun, A.; Ravelo, A. G.; Gutiérrez, D.; Giménez, D. Antiplasmodial activity of naphthoquinones related to lapachol and  $\beta$ -lapachone. *Chem. Biodiversity* **2005**, *2*, 264–274.
- (6) (a) Goulart, M. O.; Zani, C. I.; Tonholo, J.; Freitas de Abreu, F. C.; Oliveira, A. B.; Raaslan, D. S.; Starling, S.; Chiari, E. Trypanocidal activity and redox potential of heterocyclic- and 2-hydroxy-naphthoquinones. *Bioorg. Med. Chem. Lett.* **1997**, *7*, 2043–2048. (b) Ferreira, V.; Jorquiera, A.; Souza, A.; da Silva, M.; de Souza, M.; Gouvea, R.; Rodrigues, C.; Pinto, A.; Castro, H.; Santos, D.; Araujo, H.; Bourguignon, S. Trypanocidal agents with low cytotoxicity to mammalian cell line: A comparison of the theoretical and biological features of lapachone derivatives. *Bioorg. Med. Chem.* **2006**, *14*, 5459–5466.
- (7) (a) Fujiwara, A.; Mori, T.; Iida, A.; Ueda, S.; Nomura, T.; Tokuda, H.; Nishino, H. Antitumor-Promoting Naphthoquinones from *Catalpa ovata*. *J. Nat. Prod.* **1998**, *61*, 629–632. (b) Krishnan, P.; Bastow, K. F. Novel mechanisms of DNA topoisomerase II inhibition by pyranonaphthoquinone derivatives—eleutherin,  $\alpha$ -lapachone, and  $\beta$ -lapachone. *Biochem. Pharmacol.* **2000**, *60*, 1367–1379. (c) Pérez-Sacau, E.; Estévez-Braun, A.; Ravelo, A. G.; Ferro, E.; Tokuda, H.; Mukainaka, T.; Nishino, H. Inhibitory effects of lapachol derivatives on Epstein-Barr virus activation. *Bioorg. Med. Chem.* **2003**, *11*, 483–488. (d) Suzuki, M.; Amano, M.; Choi, J.; Park, H.; Williams, B.; Ono, K.; Song, C. Synergistic effects of radiation and  $\beta$ -lapachone in DU-145 human prostate cancer cells in vitro. *Radiat. Res.* **2006**, *165*, 525–531. (e) Lee, J.; Choi, D.; Chung, H.; Seo, H.; Woo, H.; Choi, B.; Choi, Y. Beta-lapachone induces growth inhibition and apoptosis in bladder cancer cells by modulation of Bcl-2 family and activation of caspases. *Exp. Oncol.* **2006**, *28*, 30–35. (f) Woo, H.; Park, K.; Rhu, C.; Lee, W.; Choi, B.; Kim, G.; Park, Y.; Choi, Y.  $\beta$ -Lapachone, a quinone isolated from *Tabebuia avellanae*, induces apoptosis in HepG2 hepatoma cell line through induction of Bax and activation of caspase. *J. Med. Food* **2006**, *9*, 161–168.
- (8) (a) Evans, B. E.; Rittle, K. E.; Bock, M. G.; Di Pardo, R. M.; Freindinger, R. M.; Whittier, W. L.; Lundell, G. F.; Veber, D. F.; Anderson, P. S.; Chang, R. S. L.; Lotte, V. J.; Cerino, D. J.; Chen, T. B.; Kling, P. J.; Kimkel, K. A.; Springer, J. P.; Hirshfield, J. Methods for drug discovery: development of potent, selective, orally effective cholecystokinin antagonists. *J. Med. Chem.* **1988**, *31*, 2235–2246. (b) Mason, J. S.; Morize, I.; Menard, P. R.; Cheney, D. L.; Hulme, C.; Labandiniere, R. F. New 4-Point Pharmacophore Method for Molecular Similarity and Diversity Applications: Overview of the Method and Applications, Including a Novel Approach to the Design of Combinatorial Libraries Containing Privileged Substructures. *J. Med. Chem.* **1999**, *42*, 3251–3264.
- (9) (a) Li, C. J.; Li, Y. Z.; Pinto, A. V.; Pardee, A. B. Potent inhibition of tumor survival in vivo by  $\beta$ -lapachone plus taxol: combining drugs imposes different artificial checkpoints. *Proc. Natl. Acad. Sci. U.S.A.* **1999**, *96*, 13369–13374. (b) Pink, J. J.; Planchon, S. M.; Tagliarino, C.; Varnes, M. E.; Siegel, D.; Boothman, D. A. NAD(P)H: quinone oxidoreductase activity is the principal determinant of  $\beta$ -lapachone cytotoxicity. *J. Biol. Chem.* **2000**, *275*, 5416–5424.
- (10) Pardee, A. B.; Li, Y. Z.; Li, C. J. Cancer therapy with  $\beta$ -lapachone. *Curr. Cancer Drug Targets* **2002**, *2*, 227–242.
- (11) Li, Y.; Sun, X.; LaMont, J. T.; Pardee, A. B.; Li, C. J. Selective killing of cancer cells by  $\beta$ -lapachone: Direct checkpoint activation as a strategy against cancer. *Proc. Natl. Acad. Sci. U.S.A.* **2003**, *100* (5), 2674–2678.
- (12) Boorstein, R. J.; Pardee, A. B. Coordinate inhibition of DNA synthesis and thymidylate synthase activity following DNA damage and repair. *Biochem. Biophys. Res. Commun.* **1983**, *117* (1), 30–36.
- (13) Li, C. J.; Averboukh, L.; Pardee, A. B.  $\beta$ -Lapachone, a novel DNA topoisomerase I inhibitor with a mode of action different from camptothecin. *J. Biol. Chem.* **1993**, *268* (30), 22463–22468.
- (14) (a) Malkinson, A. M.; Siegel, D.; Forrest, G. L.; Gazdar, A. F.; Oie, H. K.; Chan, D. C.; Bunn, P. A.; Mabry, M.; Dykes, D. J.; Harrison, S. D.; et al. Elevated DT-diaphorase activity and messenger RNA content in human non-small cell lung carcinoma: relationship to the response of lung tumor xenografts to mitomycin C. *Cancer Res.* **1992**, *52* (17), 4752–7. (b) Marin, A.; Lopez de Cerain, A.; Hamilton, E.; Lewis, A. D.; Martínez-Penuela, J. M.; Idoate, M. A.; Bello, J. DT-diaphorase and cytochrome B5 reductase in human lung and breast tumours. *Br. J. Cancer.* **1997**, *76* (7), 923–9. (c) Ough, M.; Lewis, A.; Bey, E. A.; Hinkhouse, M. M.; Ritchie, J. M.; Boothman, D. A.; Oberley, L. W.; Cullen, J. J. Efficacy of  $\beta$ -lapachone in pancreatic cancer treatment: exploiting the novel, therapeutic target NQO1. *Cancer Biol. Ther.* **2005**, *4* (1), 95–102.
- (15) Ashwell, M.; Chiang, J. L.; Tandon, M.; Liu, Y.; Lapierre, J.; Jiang, Z. Pharmaceutical compositions of beta-lapachone and beta-lapachone analogs with improved tumor targeting potential. U.S. Pat. Appl. Publ. Patent 2006034796, 2006.
- (16) Shiah, S. G.; Chuang, S. E.; Chau, Y. P.; Shen, S. C.; Kuo, M. L. Activation of c-Jun NH2-terminal kinase and subsequent CPP32/Yama during topoisomerase inhibitor  $\beta$ -Lapachone-induced apoptosis through an oxidation-dependent pathway. *Cancer Res.* **1999**, *59* (2), 391–398.
- (17) (a) Planchon, S. M.; Wuerzberger, S.; Frydman, B.; Witiak, D. T.; Hutson, P.; Church, D. R.; Wilding, G.; Boothman, D. A.  $\beta$ -Lapachone-mediated apoptosis in human promyelocytic leukemia (HL-60) and human prostate cancer cells: a p53-independent response. *Cancer Res.* **1995**, *55* (17), 3706–11. (b) Planchon, S. M.; Pink, J. J.; Tagliarino, C.; Bornmann, W.; Varnes, M. E.; Boothman, D. A.  $\beta$ -Lapachone-induced apoptosis in human prostate cancer cells: involvement of NQO1/xip3. *Exp. Cell Res.* **2001**, *267* (1), 95–106.
- (18) (a) Kurogi, Y.; Güner, O. F. Pharmacophore Modeling and Three-Dimensional Database Searching for Drug Design Using Catalyst. *Curr. Med. Chem.* **2001**, *8*, 1035–1055. (b) Güner, O.; Clement, O.; Kurogi, Y. Pharmacophore Modeling and Three-Dimensional Database Searching for Drug Design Using Catalyst: Recent Advances. *Curr. Med. Chem.* **2004**, *11*, 2991–3005.

- (19) Green, S. M.; Marshall, G. R. 3D-QSAR: A current perspective. *Trends Pharm. Sci.* **1995**, *16*, 285–291.
- (20) Klebe, G.; Abraham, U.; Mietzner, T. Molecular Similarity Indices in a Comparative Analysis (CoMSIA) of drug molecules to correlate and predict their biological activity. *J. Med. Chem.* **1994**, *37*, 4130–4146.
- (21) Ravelo, A.; Estévez-Braun, A.; Pérez-Sacau, E. The chemistry and biology of lapachol and related natural products  $\alpha$  and  $\beta$  lapachones. *Studies in Natural Products Chemistry*, Atta-Ur-Rahman, Ed.; Elsevier Science Publishers: Amsterdam, 2003, 29 (part J), 719–760 and references herein.
- (22) Seco, J. M.; Quínoa, E.; Riguera, R. The Assignment of Absolute Configuration by NMR. *Chem. Rev.* **2004**, *104*, 17–117 and references cited therein.
- (23) Pérez-Sacau, E.; Soto, J.; Estévez-Braun, A.; Ravelo, A. G. Synthesis of 9 and 10-membered macrolactones by selective ozonolysis of 1,4-diazaphenanthrene derivatives. *Tetrahedron* **2005**, *61*, 437–445.
- (24) Mosmann, T. Rapid colorimetric assay for cellular growth and survival: application to proliferation and cytotoxicity assays. *J. Immunol. Methods* **1983**, *65*, 55–63.
- (25) Fischer, R. The Principle of Experimentation, Illustrated by a Psycho-Physical Experiment. In *The Design of Experiments*, 8th ed.; Hafner Publishing Co.: New York, 1966; Chapt. II.
- (26) Silva, M. S.; Camara, C. A.; Barbosa, T. P.; Soares, A. Z.; da Cunha, L. C.; Pinto, A. C.; Vargas, M. D. Molluscicidal activity of synthetic lapachol amino and hydrogenated derivatives. *Bioorg Med. Chem.* **2005**, *13* (1), 193–196.
- (27) (a) Gupta, R. B.; Khanna, R. N. Bromination with *N*-bromosuccinimide: Part II. An unusual dibromination of  $\beta$ -lapachone to 3',4'-dibromo- $\beta$ -lapachone. *Indian J. Chem., Sect. B* **1980**, *19B* (1), 13–16. (b) Gupta, R. B.; Khanna, R. N. Bromination with *N*-bromosuccinimide: Part III. Formation of 3'-bromo- $\beta$ -lapachone, dehydro-iso- $\beta$ -lapachone and 4'-bromo-iso- $\beta$ -lapachone from lapachol. *Indian J. Chem., Sect. B* **1980**, *19B* (1), 17–19. (c) Kapoor, N. K.; Gupta, R. B.; Khanna, R. N. Reaction of lapachol with lead tetraacetate and *N*-bromosuccinimide. *Indian J. Chem., Sect. B* **1981**, *20B* (6), 508–509.
- (28) Sun, J. S.; Geiser, A. H.; Frydman, B. A preparative synthesis of lapachol and related naphthoquinones. *Tetrahedron Lett.* **1998**, *39* (45), 8221–8224.
- (29) Gallagher, R.; Collins, S.; Trujillo, J.; McCredie, K.; Ahearn, M.; Tsai, S.; Metzgar, R.; Aulakh, G.; Ting, R.; Ruscetti, F.; Gallo, R. Characterization of the continuous, differentiating myeloid cell line (HL-60) from a patient with acute promyelocytic leukemia. *Blood* **1979**, *54* (3), 713–733.
- (30) Mosmann, T. Rapid colorimetric assay for cellular growth and survival: application to proliferation and cytotoxicity assays. *J. Immunol. Methods* **1983**, *65*, 55–63.
- (31) De Lean, A.; Munson, P. J.; Rodbard, D. Simultaneous analysis of families of sigmoidal curves: application to bioassay, radioligand assay, and physiological dose–response curves. *Am. J. Physiol.* **1978**, *235*, E97–E102.
- (32) Li, H.; Sutter, J.; Hoffmann, R. *Int. Univ. Line: La Jolla* **2000**, 174–189.
- (33) Singh, U. C.; Kollman, P. A. An approach to computing electrostatic charges for molecules. *J. Comput. Chem.* **1984**, *5*, 129–145.
- (34) Hawkins, G. D.; Giesen, D. J.; Lynch, G. C.; Chambers, C. C.; Rossi, I.; Storer, J. W.; Li, J.; Zhu, T.; Winget, P.; Rinaldi, D.; Liotard, D. A.; Cramer, C. J.; Truhlar, D. G. AMSOL 6.7.2; University of Minnesota, Minneapolis, MN 55455–0431.
- (35) Böhm, M.; Stürzebecher, J.; Klebe, G. Three-dimensional quantitative structure–activity relationship analyses using comparative molecular field analysis and comparative molecular similarity indices analysis to elucidate selectivity differences of inhibitors binding to trypsin, thrombin, and factor Xa. *J. Med. Chem.* **1999**, *42*, 458–477.
- (36) (a) Dunn, W. J. I.; Wold, S.; Edlund, U.; Hellberg, S.; Gasteiger, J. Multivariate structure–activity relationships between data from a battery of biological tests and an ensemble of structure descriptors: The PLS method. *Quant. Struct.-Act. Relat.* **1984**, *3*, 131–137. (b) Wold, S.; Ruhe, A.; Wold, H.; Dunn, W. J. I. The covariance problem in linear regression. The partial least squares (PLS) approach to generalized inverses. *SIAM J. Sci. Stat. Comput.* **1984**, *5*, 735–743. (c) Wold, S.; Albano, C.; Dunn, W. J. I.; Edlund, U.; Esbensen, W.; Geladi, P.; Hellberg, S.; Johansson, E.; Lindberg, W.; Sjöström, M. Multivariate data analysis in chemistry. In *Chemometrics: Mathematics and Statistics in Chemistry*; Kowalsky, B. R., Ed.; Reidel: Dordrecht, The Netherlands, 1984; pp 17–95. (d) Cramer, R. D.; Bunce, J. D.; Patterson, D. E. Crossvalidation, bootstrapping and partial least squares compared with multiple regression in conventional QSAR studies. *Quant. Struct.-Act. Relat.* **1988**, *7*, 18–25.
- (37) SYBYL 7.0; Tripos Inc., 1699 South Hanley Rd., St. Louis, MO 63144.

JM060849B